energy&fuels

pubs.acs.org/EF

Article

Autoignition Characteristics of Ammonia Dimethyl Ether Blends

Tushar Goyal and Omid Samimi-Abianeh*

Cite This: https://doi.org/10.1021/acs.energyfuels.4c01157

Read Online

ACCESS | Metrics & More | Article Recommendations | Supporting Information

ABSTRACT: The autoignition characteristics of ammonia (NH_3) and dimethyl ether (DME) blends were examined in this research project. The study investigates the autoignition characteristics by measuring ignition delay times across a range of gas temperatures from 621 to 725 K and at pressures of 5, 10, and 20 bar by using a rapid compression machine (RCM). Ignition delays of NH_3/DME blends, with DME concentrations in the fuel mixture ranging from 0 to 50%, were measured, simulated, and compared with JP-8 and JP-5 fuel ignition delays. At a pressure of 20 bar, blends containing 30 and 50% DME concentrations exhibited ignition delay times similar to those of JP-8 and JP-5. Furthermore, the fuel blend with a 30% DME concentration showed similar ignition delays at the lower pressures of 5 and 10 bar. Several kinetic models were used to model the autoignition and compared with the measured data. Simulation results fairly matched the measured ignition delays. Through rigorous experimental verification, this comprehensive analysis evaluated the reliability of existing chemical models and paved the way for further studies on customized fuel blends, thereby contributing to the ongoing debate on sustainable energy alternatives.

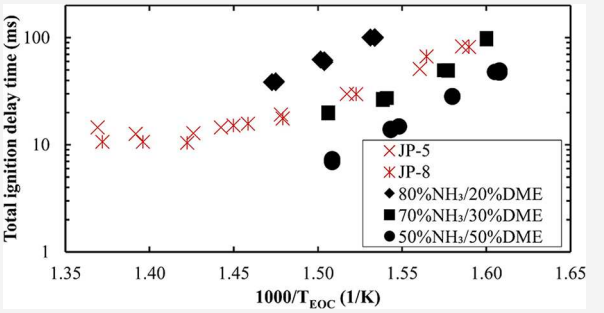

1. INTRODUCTION

The urgent need to reduce carbon emissions in the aviation sector has spurred the search for sustainable alternatives to conventional jet fuels. Blends of ammonia (NH_3) and dimethyl ether (DME) have emerged as promising contenders, offering the potential for high energy density and clean combustion. This study delves into the autoignition characteristics of NH_3/DME blends, assessing their suitability as replacements for established jet fuels, such as JP-8 and JP-5. By utilizing a rapid compression machine (RCM), the research analyzes ignition delay times under various thermodynamic conditions, a crucial step in determining the practicality of these blends in real-world aviation applications. While ammonia is known for its carbon-neutral combustion, it faces challenges due to low burn rates and high NOx emissions. On the other hand, DME boasts excellent combustion features, including short ignition delay and high cetane numbers, making it a potential copromoter with NH_3 to enhance operational performance. This section provides a concise overview of key studies supporting this research.

Autoignition characteristics of NH_3/DME blends across a wide range of gas temperatures (610−1180 K), DME concentrations (0, 2, 5, and 100% DME in the fuel mixture), equivalence ratios (0.5, 1.0, and 2.0), and pressures (10−70 bar) were experimentally investigated using RCM.[1] The authors showed that increasing the DME concentration markedly reduced ignition delay times. In addition, a two-stage ignition phenomenon was observed for equivalence ratios of 1.0 and 2.0 for 2% and 5% DME concentrations under high pressures. Furthermore, the authors developed an NH_3/DME kinetic model to predict ignition delays accurately. The simulation showed the role of the low-temperature chain-branching reactions of DME and the critical role of specific cross-reactions between DME and NH_3 species in the ignition process, even at low DME concentrations in the total fuel mixture.

Issayev et al.[2] investigated the autoignition characteristics to highlight DME's impact on NH_3's ignition behavior. The experiments were conducted across a wide range of gas temperatures (649−950 K), pressures of 20 and 40 bar, and varying equivalence ratios (0.5 and 1) with DME concentrations in the fuel mixture ranging from 0.05 to 0.5 using RCM. The authors showed that at a DME composition of 10%, the NH_3/DME blend approximated the low-temperature autoignition characteristics of gasoline under specific conditions (20 bar, stoichiometric mixture). The authors observed that increasing the DME concentration to 18% could mimic a research octane number of approximately 95. In addition, the authors found blends with higher DME concentrations (40−50%) nearly mimicked the ignition behavior of pure DME, making them suitable for compression−ignition engines.

Received: March 12, 2024
Revised: May 24, 2024
Accepted: May 28, 2024

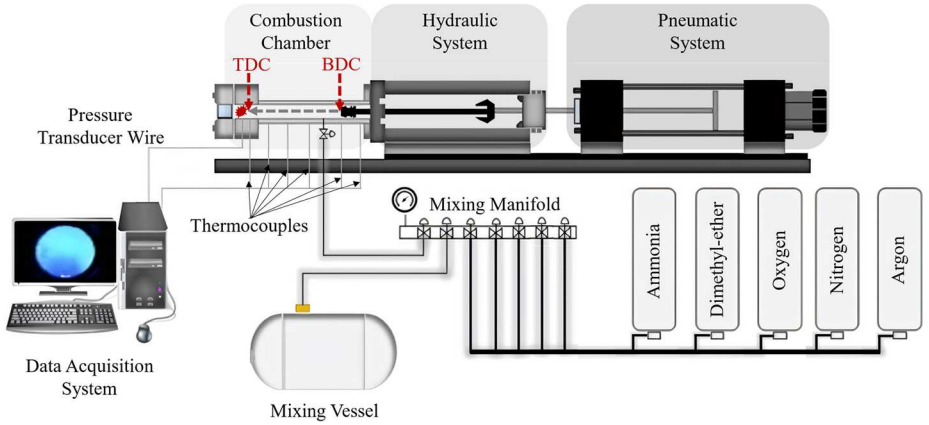

Figure 1. Schematic of the RCM.

Moreover, the authors observed a pronounced dependence of pressure on ignition delay times at lower DME concentrations in the fuel mixture, which diminished with higher concentrations and increasing pressure.

The effects of DME on NH_3 ignition behavior were investigated behind reflected shock waves by Jin et al.[3] The experiments were conducted at pressures of 0.14 and 1.0 MPa and gas temperatures ranging from 1150 to 1950 K. Different equivalence ratios of 0.5, 1.0, and 2.0, and NH_3/DME mixing ratios of 100/0, 95/5, 90/10, and 70/30 were investigated. The authors showed that NH_3's reactivity was increased with an increase in the DME concentration. Furthermore, the authors refined the Shrestha−Burke kinetic mechanism and closely matched the experimental data. The simulation results indicated that the DME facilitated early radical formation during ignition, with a marked dependency on the temperature and pressure, especially at lower temperatures and higher pressures.

Combustion characteristics of DME/NH_3 blends with 0, 20, and 40% NH_3 concentrations were investigated using a compression−ignition engine.[4] The authors observed that increasing the NH_3 concentration caused a longer ignition delay. The study also showed that incorporating NH_3 into the total fuel mixture reduced the combustion temperature, which led to an increase in CO and HC emissions. NOx emissions were found to be higher for blends with higher NH_3 concentrations, i.e., above 20%.

A numerical study was conducted to investigate the combustion and emission characteristics of NH_3/DME blends, utilizing a detailed kinetic model including 221 species and 1597 reactions.[5] The mechanism developed was validated for autoignition characteristics under various initial conditions, with equivalence ratios ranging from 0.5 to 2 and pressures from 12 to 25 bar. The results showed NOx (due to the fuel nitrogen component) as the primary source of total NOx emission. The authors found that ammonia primarily consumed O, H, and OH, producing NH_2 radicals, and NO was produced from HNO and NO_2.

Despite these efforts, a noticeable gap remains in our comprehension of the ignition delays of NH_3/DME blends under conditions resembling those of conventional aviation fuels, especially at elevated temperatures and pressures. The autoignition characteristics and chemical kinetics of fuel typically vary with temperature; therefore, expanding the ignition delay research on NH_3/DME across a wider temperature spectrum is essential to aid both practical implementation and kinetic model validation. Thus, this study seeks to bridge this gap by evaluating stoichiometric NH_3/DME blends' autoignition across blending ratios (10, 20, 30, and 50% DME in the fuel mixture) and pressures of 5, 10, and 20 bar. In addition, the investigation includes validating chemical kinetic models over a wide range of elevated gas temperatures and pressures. Furthermore, the study analyzes the ratio of the first stage to total ignition delay in understanding whether the reactivity of the blend alternated between rate-determining and chemistry-controlling ignition phenomenon is discussed.

2. EXPERIMENTAL SETUP

The details of the experimental setup had been published by authors in previous works.[6−8] In the following section, a brief overview of the setup is provided. The experimental setup was similar to previous studies, utilizing an RCM with a 2-in. bore and 10-in. stroke combustion chamber, as shown in Figure 1. Pneumatic and hydraulic systems, a stainless-steel vessel for gas premixing, and a pressure and temperature measurement system supplemented this combustion chamber. Gas temperature was precisely measured by an Omega K-type thermocouple (KMQSS-125G-6, with an associated uncertainty of ±1.1 K). The premixed gas temperature was measured at 298 K with an accuracy of ±1.1 K. Additionally, the uniformity of the chamber wall temperatures was monitored using five Omega K-type thermocouples (KMQSS-062G-6, each with an uncertainty of ±2.2 K). The compression ratio was fixed at 8 by adjusting the clearance spacers behind the creviced piston, and the duration of the compression stroke varied between 30 and 55 ms based on the pneumatic pressure applied. This approach was adopted to minimize the boundary layer vortex induced by piston movement, ensuring homogeneous conditions within the combustion chamber throughout the experiments. Pressure data before and after compression in each autoignition trial were acquired using a Kistler 6045B piezoelectric pressure transducer (with an uncertainty of 0.56%), connected to a Kistler 5018 charge amplifier, and the data were logged via a program developed in NI LabVIEW.

High-purity gases were sourced, including argon (Ar, 99.9999%), nitrogen (N_2, 99.9999%), oxygen (O_2, 99.9999%), and ammonia (NH_3, 99.999%), all obtained from Airgas, and dimethyl ether (DME or CH_3OCH_3, 99.5%) acquired from BVV. Before each experimental series, the mixture was prepared in a 5-gallon stainless-steel vessel, initially evacuated to a subatmospheric pressure of 2 mbar using an Agilent vacuum pump (DS202). The pressure during mixture preparation was precisely monitored using an Omega static pressure sensor (PX409-050A10 V-EH) with an accuracy of ±0.05% of the reading. Following the preparation, the test mixture was allowed to stabilize overnight to ensure uniform homogeneity.

https://doi.org/10.1021/acs.energyfuels.4c01157
Energy Fuels XXXX, XXX, XXX−XXX

Before initiating each experiment, the residual gases that remained within the RCM's combustion chamber were evacuated using the vacuum pump, reaching a subatmospheric pressure of 2 mbar. Subsequently, test mixtures prepared in a stainless-steel vessel were introduced into the chamber to a desired initial pressure. A waiting period of about 5 min was incorporated to allow the mixture to achieve thermal equilibrium and a quiescent condition within the chamber, without any flow activity, following the filling operation. Note that in experiments resulting in longer ignition delay times (>100 ms) with mixtures containing only argon as an inert gas, the RCM chamber was heated up using five evenly spaced heating bands. The gas and wall temperatures were monitored using the previously mentioned thermocouples and regulated using an NI LabVIEW program. Figure 2 presents a collection of several pressure−time

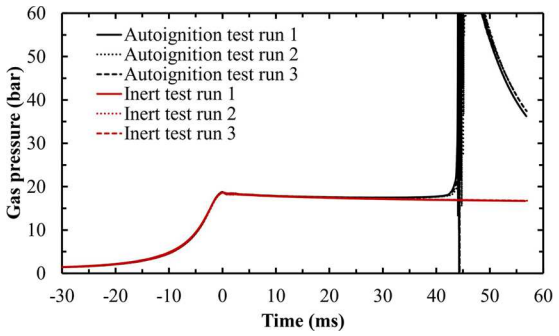

Figure 2. Pressure−time histories of autoignition and inert tests from three experiments of an NH3/DME blend, D_{30-N30}, as shown in Table 1, illustrating repeatability. The experiments were conducted at a gas pressure of 20 bar and a temperature of 636 K.

traces obtained under the experimental conditions, demonstrating the repeatability of the experimental measurements used in this study. To ensure the accuracy of the data, each experimental condition was performed at least three times.

The experiments covered a range of mixture compositions, as outlined in Table 1. The subscripts "N00" to "N30" denoted the mole fraction of nitrogen in the $O_2/N_2/Ar$ mixture (i.e., 0, 10, 20, and 30%). For example, blend D_{50-N10} corresponded to 50% DME in the fuel mixture with 10% nitrogen in the $O_2/N_2/Ar$ mixture. The dilution rate for all experiments was kept at 79%. The DME blending ratio (D_R) was calculated as the mole fraction of DME (χ_{DME}) relative to the total fuel mixture $\left(\frac{\chi_{DME}}{\chi_{NH_3}+\chi_{DME}}\right)$.

The ignition delay time was determined based on the pressure−time history obtained during the autoignition experiments, as shown in Figure 3. The first-stage ignition delay (τ_1) was defined as the duration between the end of compression (EOC) and the time when

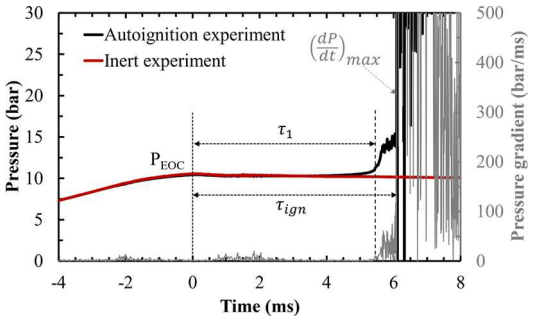

Figure 3. Pressure and pressure gradient of D_{50-N10} mixture (as shown in Table 1) at the gas pressure and gas temperature of 10 bar and 663 K. The reference point of time 0 ms corresponds to the EOC.

the first peak of a pressure gradient was reached. The total ignition delay (τ_{ign}) was defined as the duration between the EOC and the time of the maximum peak of the pressure gradient (τ_{ign}). The temperature−time history was derived from the recorded pressure by employing an isentropic relation given by eq 1,

$$\ln\left(\frac{P_{EOC}}{P_i}\right) = \int_{T_i}^{T_{EOC}} \frac{\gamma(T)}{\gamma - 1}\frac{dT}{T} \quad (1)$$

where the subscripts "i" and "EOC" denote the initial and EOC conditions, respectively; "T" and "P" refer to the temperature and pressure, and $\gamma(T)$ is the temperature-dependent specific heat capacity ratio of the core gas. Throughout the article, the end of the compression pressure and the end of the compression gas temperature are referred to as the gas pressure and gas temperature.

3. NUMERICAL SIMULATIONS

The details of the numerical setup have been published by authors in previous works[6,9,10] However, a brief overview is provided in this section. Numerical simulations of ignition delays were performed in a zero-dimensional homogeneous batch reactor (0-D HBR) model, employing the Chemkin-Pro software suite.[11] Five kinetic models, tailored for NH_3/DME blended mixtures, were used to simulate and validate ignition delay times under the studied conditions. Table 2 shows the details of the kinetic mechanisms.

To account for heat transfer from gas to the chamber wall and compression stroke, nonreactive (or inert) experiments were performed under the same conditions as their reactive mixture counterparts, given the analogous thermodynamic properties. The nonreactive pressure−time histories obtained were utilized to produce volume−time profiles, employing

Table 1. Mixture Composition[a]

mixture no.	mixture name	$D_{R-N\%}$	χ_{NH3}	χ_{DME}	χ_{O_2}	χ_{N_2}	χ_{Ar}
1	D_{50}	D_{50-N00}	0.0504	0.0504	0.1888		0.7104
2		D_{50-N10}				0.0710	0.6394
3		D_{50-N20}				0.1421	0.5683
4		D_{50-N30}				0.2131	0.4973
5	D_{30}	D_{30-N00}	0.0899	0.0385	0.1830		0.6885
6		D_{30-N10}				0.0689	0.6197
7		D_{30-N20}				0.1377	0.5508
8		D_{30-N30}				0.2066	0.4820
9	D_{20}	D_{20-N00}	0.1192	0.0298	0.1787		0.6723
10		D_{20-N10}				0.0672	0.6051
11	D_{10}	D_{10-N00}	0.1595	0.0177	0.1728		0.6500

[a]The mole fractions of the mixture components are reported.

https://doi.org/10.1021/acs.energyfuels.4c01157
Energy Fuels XXXX, XXX, XXX−XXX

Table 2. Details of the Kinetic Mechanisms Used

mechanism no.	kinetic model	abbreviation	species	reactions	refs
1	Dai et al. Mech	MD	191	1657	1
2	Issayev et al. Mech	MI	176	1418	2
3	Zhang et al. Mech	MZ	108	616	12
4	Murakami et al. Mech	MM	234	1685	13
5	Xiao et al. Mech	MX	102	594	14

temperature-dependent specific heat capacity ratios. Following the derivation of the volume−time trace, the initial experimental conditions were used in the 0-D HBR model to simulate autoignition. The details can be found in ref 15. Figure 4 showcases a combination of the measured and

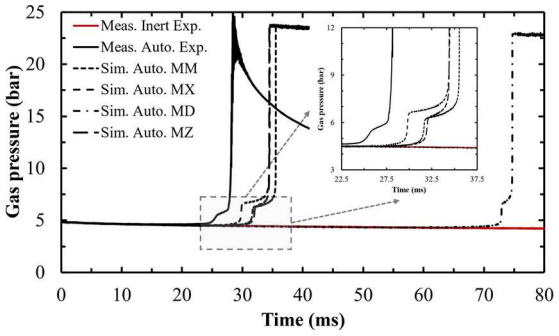

Figure 4. Pressure−time histories of a stoichiometric D_{50-N20} mixture depicted under reactive (autoignition) mixture (black lines) and nonreactive (inert) mixture (red lines) stated at the gas temperature of 636 K and pressure of 5 bar. The profiles were simulated using volume-time data generated with a 0-D HBR model. The abbreviations refer to the kinetic models described in Table 2, with the time origin set at 0 ms, corresponding to the EOC position.

simulated autoignition pressure profiles for a stoichiometric NH_3/DME blend (D_{50-N20}), observed under both autoignition and inert conditions at the gas pressure of 5 bar and temperature of 636 K. Ignition delay times predicted by mechanisms MM, MX, and MZ closely mirrored the experimental data across a majority of the tested conditions, also capturing key ignition features such as multistage ignition delays. These mechanisms underpredicted ignition delay in comparison to the experimental data. While MD notably overestimates ignition delays across the evaluated conditions. Mechanism MI could not generate pressure profiles under certain conditions (e.g., as shown in Figure 4). Mechanisms MM, MX, and MZ were considered to provide a relatively good depiction of the autoignition behavior of the NH_3/DME blends. However, by comparing the simulated and measured ignition delays under various conditions, the simulated results using mechanism MZ (Zhang et al.) were selected and shown in the paper.

4. RESULTS AND DISCUSSION

Parametric analyses were conducted to characterize the autoignition characteristics of four NH_3/DME blends (as referenced in Table 1) across a wide range of temperatures (621−725 K) and three pressures (5, 10, and 20) and at an equivalence ratio of 1.0. Figures 5 and 10 show the ignition delays in an Arrhenius-type plot, depicting the logarithm of ignition delay against the inverse of the gas temperature

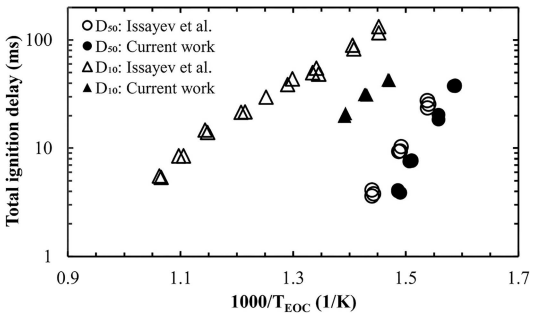

Figure 5. Measured total ignition delay in the current work and data from the literature. Hollow symbols represent experimental data sourced from Issayev et al.,[2] employing an O2/N2 oxidizing mixture. In contrast, the present study (solid symbols) utilizes an O2/N2/Ar mixture for oxidation (see Table 1). Measurements were conducted at a gas pressure of 20 bar.

(T_{EOC}). All the literature reviews and experimental data of the current work are documented tabularly in the Supporting Information.

Figure 5 shows a comparative analysis of ignition delay times from the current study, and those reported by Issayev et al.[2] conducted at a gas pressure of 20 bar and an equivalence ratio of 1.0. Notably, the data align closely for NH_3/DME blends with higher DME concentrations, such as the D_{50} blend. However, a pronounced difference is evident in the blend with a lower DME content, particularly the D_{10} blend. For both mixtures, the current measured ignition delays are shorter than the one measured by Issayev et al. The authors speculate that this behavior is due to the lower pressure drop during the postcompression of current work with respect to Issayev et al. The RCM heat transfer characteristic is a function of the mixture composition, RCM chamber size, and shape, as discussed in our previous work.[10] In addition, it should be noted that Issayev et al. used nitrogen as a diluent, and a mixture of nitrogen and argon was used in the current work, which could cause different heat transfer characteristics. The nonreacting mixture pressure−time histories for all the tested mixtures are provided in the Supporting Information to make the data usable and verifiable by researchers and kinetic model developers.

Figure 6 shows the measured ignition delay times of four NH_3/DME mixtures, tested at a gas pressure of 5 bar and an equivalence ratio of 1.0. Among the blends studied, the D_{30} blend mirrored the ignition delays of JP-8 and JP-5, measured by Casey et al.[16] (JP-8, POSF-6169), Casey et al.[17] (JP-5, Naval jet fuel), and Narayanaswamy et al.[18] (JP-8, POSF-6169). In contrast, the D_{20} blend exhibited longer ignition delay times compared to JP-8 and JP-5 across all conditions. This highlights the lower DME content reaching a threshold where insufficient intermediate pool enrichment hinders ignition kinetics. Furthermore, the D_{50} blend displayed shorter ignition delay times than the jet fuels. D_{10} blend failed to autoignite entirely at the set gas pressure and temperatures.

Figures 7 and 8 show the measured ignition delays for jet fuels JP-8 and JP-5 versus four NH_3/DME blends at gas pressures of 10 and 20 bar. Details of the experimental data, operational conditions, and composition for JP-8 and JP-5 are explained in refs 16−19. In these studies, the JP-8 (POSF-6169) fuel was from the Air Force Research Laboratory at Wright Patterson Air Force Base, and JP-5 was from the NAVAIR Naval Fuels and Lubricants Cross-Functional Team.

https://doi.org/10.1021/acs.energyfuels.4c01157
Energy Fuels XXXX, XXX, XXX−XXX

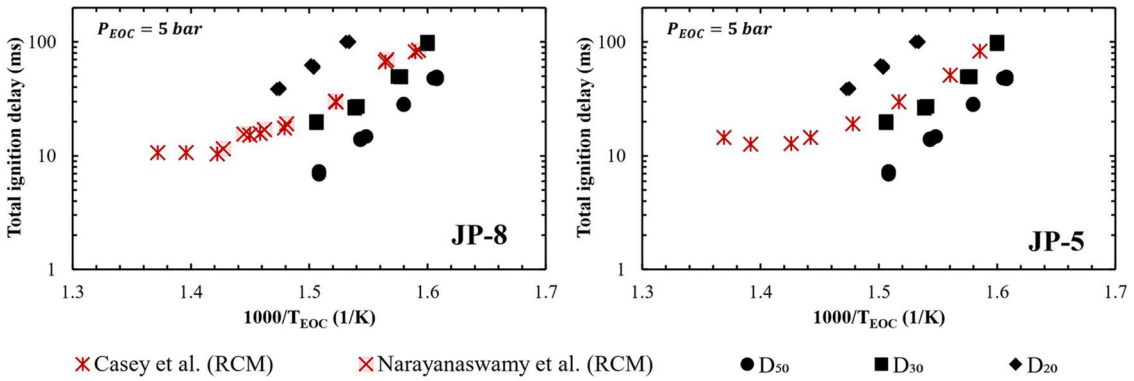

Figure 6. Ignition delay times for three NH3/DME blends (black symbols, current work) against those for aviation fuels JP-8 and JP-5. The JP-8 data are from Casey et al.[16] and Narayanaswamy et al.[18] (on the left), while the JP-5 data are from Casey et al.[17] (on the right). The comparisons are conducted at a gas pressure of 5 bar and an equivalence ratio of 1.0.

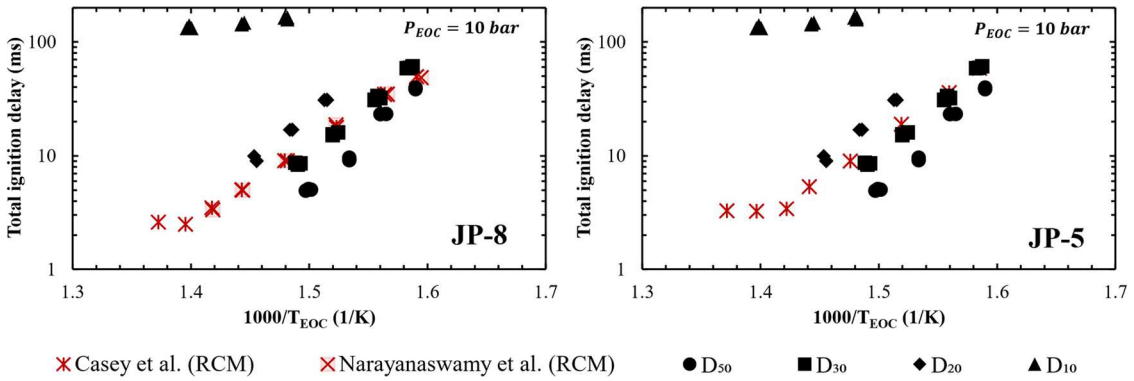

Figure 7. Ignition delay times of four NH3/DME blends (black symbols, current work) against those for aviation fuels JP-8 and JP-5. The JP-8 data are from Casey et al.[16] and Narayanaswamy et al.[18] (on the left), while the JP-5 data are from Casey et al.[17] (on the right).

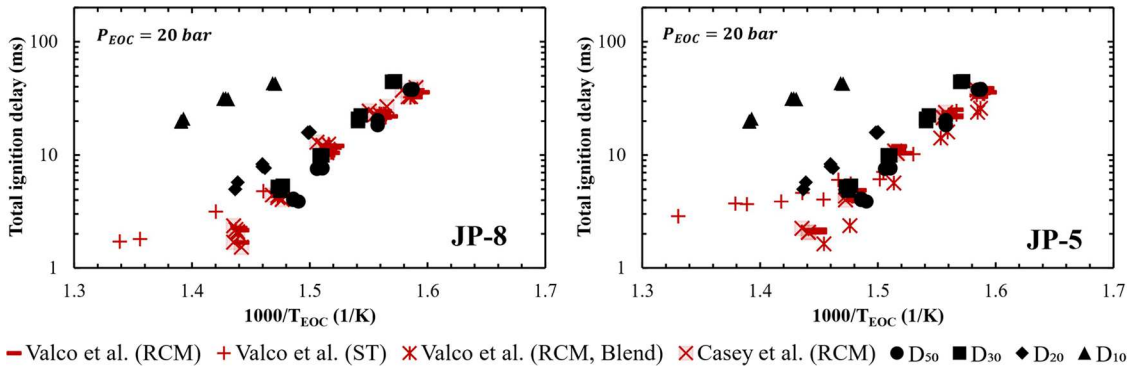

Figure 8. Ignition delay times for four NH3/DME blends (black symbols, current work) against those for aviation fuels JP-8 and JP-5. The JP-8 data are from Casey et al.[16] and Valco et al.[19] (on the left), while the JP-5 data are from Casey et al.[17] and Valco et al.[19] (on the right).

At 10 bar, both D_{30} and D_{50} blends show a good agreement with JP fuel ignition delay times at lower temperatures. However, with the rising temperatures, the results indicated that the mixture containing the D_{50} blend diverges away from the JP fuel ignition delays. This difference in ignition delays can be attributed to the faster reaction rate shifting the dominance from the thermal decomposition of NH_3 toward the combustion of DME itself, leading to the relative radical contribution from NH_3.[2] At 20 bar pressure, the difference between D_{20}, D_{30}, and D_{50} mixture ignition delays become smaller.

Figure 9 shows the measured and simulated first-stage ignition delays of four NH_3/DME blends at gas pressures of 5, 10, and 20 bar. It was observed across all autoignition experiments that the ignition process exhibited a two-stage behavior. Notably, in certain cases, the duration between the first-stage ignition and total ignition delay is less than 1.0 ms. The first-stage ignition delay times decrease with increasing gas pressures and show linear trends across the temperature spectrum. Simulations of the first-stage ignition delays align with this experimental trajectory, overpredict ignition delays, with notable differences at the lower pressures of 5 and 10 bar.

Figure 10 shows the measured and simulated total ignition delays for four stoichiometric NH_3/DME blends at gas pressures of 5, 10, and 20 bar. The total ignition delay times decrease with increasing gas pressure. The mechanism predicts

https://doi.org/10.1021/acs.energyfuels.4c01157
Energy Fuels XXXX, XXX, XXX−XXX

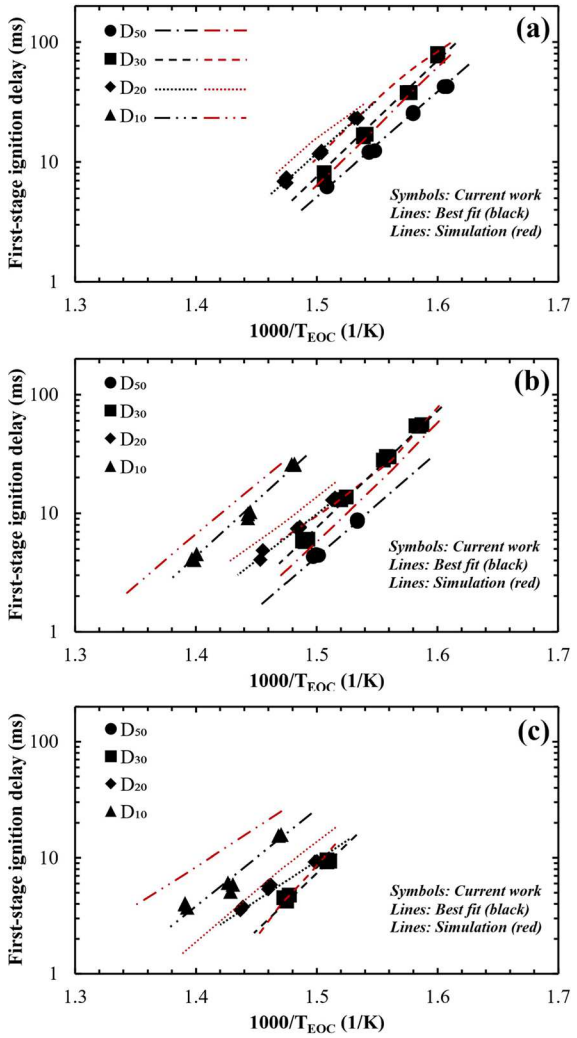

Figure 9. First-stage ignition delay at three gas pressures of (a) 5, (b) 10, and (c) 20 bar. D_{50}, D_{30}, D_{20}, and D_{10} are the NH3/DME blends, as reported in Table 1.

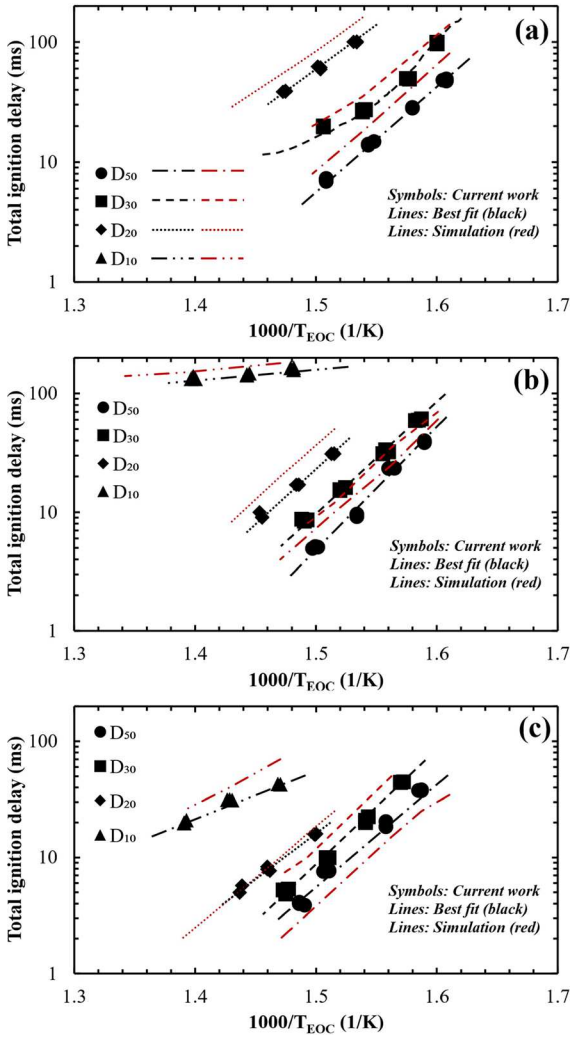

Figure 10. Total ignition delay at three gas pressures of (a) 5, (b) 10, and (c) 20 bar. D_{50}, D_{30}, D_{20}, and D_{10} are the NH3/DME blends, as reported in Table 1.

the total ignition delay well enough. However, the observed timing of the simulated total ignition delay was slightly longer than that of the measured data.

To understand the rate-determining and chemistry-controlling ignition phenomena for NH_3/DME blends, the ratio of the first-stage ignition delay to the total ignition delay time was calculated and is shown in Figure 11. In general, the first-stage delay encompasses the low-temperature reactions involving chain initiation, propagation, and branching to build up a pool of reactive radicals and intermediates. Subsequently, the second stage involves high-temperature oxidation reactions that consume these intermediates, leading to autoignition. Analysis of Figure 11 revealed that blend D_{50} exhibited a higher first-to-total ignition delay ratio, highlighting the dominance of the early-stage kinetics in governing the timeline of the ignition process. However, a reduction in the DME mole fractions, particularly in the D_{30} blend, resulted in a nonlinear decrease in this ratio.

5. CONCLUSIONS

This study investigated the autoignition characteristics of NH_3/DME fuel blends compared with traditional aviation fuels such as JP-8 and JP-5. Through experimentation, first-stage and total ignition delay times were measured for four NH_3/DME blends with 10, 20, 30, and 50% DME concentrations in the fuel mixture. These measurements were conducted using an RCM under stoichiometric conditions, spanning a gas temperature range of 621−725 K and 5, 10, and 20 bar pressures. A homogeneous batch reactor model was used to simulate the ignition delay using several kinetic models. The heat transfer model of the RCM was developed and utilized in the HBR model. Simulation results from the Zhang model predict the measured ignition delay fairly well.

The results highlighted that adding DME to NH_3 decreases the ignition delay, even at the lowest concentration tested. Particularly, the D_{30} and D_{50} blends showed autoignition characteristics similar to those of JP-8 and JP-5 under high-pressure (20 bar) conditions. At lower pressures (5 and 10 bar), the D_{30} blend shows ignition delays similar to those of jet fuels.

The experiments showed two-stage ignition behavior under most of the studied conditions. The first-stage ignition delay times showed a decrease with increasing gas pressure and increasing DME concentration in the fuel mixture. The simulation and measured first-stage ignition delay agreed fairly

https://doi.org/10.1021/acs.energyfuels.4c01157
Energy Fuels XXXX, XXX, XXX−XXX

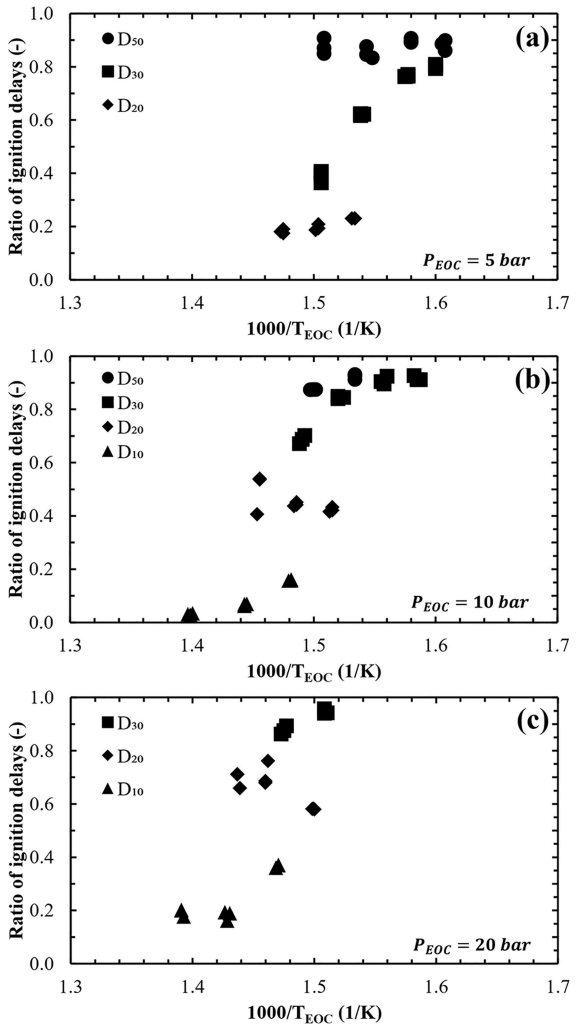

Figure 11. Ratio of first-stage to total ignition delays at three gas pressures of (a) 5, (b) 10, and (c) 20 bar. D_{50}, D_{30}, D_{20}, and D_{10} are the NH3/DME blends as reported in Table 1. The ratio of ignition delays (*Y*-axis) is the ratio of the first-stage ignition delay to the total ignition delay.

well; however, notable differences were observed at lower pressures (i.e., 5 and 10 bar), as the simulated first-stage ignition delay times were slightly longer than the measured data. Similarly, the total ignition delay showed a decrease with increasing gas pressure and increasing DME concentration in the total fuel mixture. The total ignition delay simulation results were longer than the measured data.

■ ASSOCIATED CONTENT

Supporting Information

The Supporting Information is available free of charge at https://pubs.acs.org/doi/10.1021/acs.energyfuels.4c01157.

Summary of existing and current works' experimental data, pressure−time profiles for autoignition, and inert experiments for the studied conditions (XLSX)

■ AUTHOR INFORMATION

Corresponding Author

Omid Samimi-Abianeh − *Department of Mechanical Engineering, Wayne State University, Detroit, Michigan 48202, United States;* orcid.org/0000-0002-6931-4433; Email: O.Samimi@wayne.edu

Author

Tushar Goyal − *Department of Mechanical Engineering, Wayne State University, Detroit, Michigan 48202, United States*

Complete contact information is available at: https://pubs.acs.org/10.1021/acs.energyfuels.4c01157

Notes

The authors declare no competing financial interest.

■ ACKNOWLEDGMENTS

This material is based upon work supported by the United States National Science Foundation (NSF) under Grant No. 2324471.

■ REFERENCES

(1) Dai, L.; Hashemi, H.; Glarborg, P.; Gersen, S.; Marshall, P.; Mokhov, A.; Levinsky, H. Ignition Delay Times of NH3/DME Blends at High Pressure and Low DME Fraction: RCM Experiments and Simulations. *Combust. Flame* **2021**, *227*, 120−134.

(2) Issayev, G.; Giri, B. R.; Elbaz, A. M.; Shrestha, K. P.; Mauss, F.; Roberts, W. L.; Farooq, A. Ignition Delay Time and Laminar Flame Speed Measurements of Ammonia Blended with Dimethyl Ether: A Promising Low Carbon Fuel Blend. *Renew. Energy* **2022**, *181*, 1353−1370.

(3) Jin, Y.; Li, X.; Wang, X.; Ma, Z.; Chu, X. Effect of Dimethyl Ether on Ignition Characteristics of Ammonia and Chemical Kinetics. *Fuel* **2023**, *343*, No. 127885.

(4) Gross, C. W.; Kong, S. C. Performance Characteristics of a Compression-Ignition Engine Using Direct-Injection Ammonia-DME Mixtures. *Fuel* **2013**, *103*, 1069−1079.

(5) Meng, X.; Zhang, M.; Zhao, C.; Tian, H.; Tian, J.; Long, W.; Bi, M. Study of Combustion and NO Chemical Reaction Mechanism in Ammonia Blended with DME. *Fuel* **2022**, *319*, No. 123832.

(6) Zyada, A.; Samimi-Abianeh, O. Ethanol Kinetic Model Development and Validation at Wide Ranges of Mixture Temperatures, Pressures, and Equivalence Ratios. *Energy Fuels* **2019**, *33* (8), 7791−7804.

(7) Molana, M.; Goyal, T.; Samimi-Abianeh, O. Measurement and Simulation of N-Heptane Mixture Autoignition. *Ind. Eng. Chem. Res.* **2021**, *60* (38), 13859−13868.

(8) Piehl, J. A.; Samimi-Abianeh, O. Species Quantification during N-Heptane Autoignition Using Filtered Natural Emission of Species. *Fuel* **2021**, *305*, No. 121563.

(9) Samimi Abianeh, O.; Chen, C. P.; Cerro, R. L. Mass Transfer and Conservation from a Finite Source to an Infinite Media. *Int. J. Chem. React. Eng.* **2013**, *11* (2), 657−666.

(10) Samimi-Abianeh, O. Autoignition of Reacting Hydrocarbon Mixture with Negative Temperature Coefficient Due to the Cold-Spot and Cold Chamber Wall. *J. Energy Resour. Technol.* **2022**, *144*, No. 062305, DOI: 10.1115/1.4052671.

(11) ANSYS, I. *CHEMKIN-PRO 2020 R2, Theory Manual*; 2020.

(12) Zhang, Y.; Wang, Q.; Dai, L.; Zhang, M.; Yu, C. Numerical Study on the Combustion Properties of Ammonia/DME and Ammonia/DMM Mixtures. *Energies* **2023**, *16* (19), 6929.

(13) Murakami, Y.; Nakamura, H.; Tezuka, T.; Hiraoka, K.; Maruta, K. Effects of Mixture Composition on Oxidation and Reactivity of DME/NH3/Air Mixtures Examined by a Micro Flow Reactor with a Controlled Temperature Profile. *Combust. Flame* **2022**, *238*, No. 111911.

(14) Li, H.; Xiao, H. Experimental Study on the Explosion Characteristics of NH3/DME/Air Mixtures. *Fuel* **2023**, *352*, No. 129069.

(15) Piehl, J. A.; Samimi-Abianeh, O. Measuring the Adiabatic Ignition Delay of N-Pentane Mixture Using Rapid Compression Machine. *J. Therm. Sci.* **2022**, *31* (2), 552−560.
(16) Allen, C.; Valco, D.; Toulson, E.; Edwards, T.; Lee, T. Ignition Behavior and Surrogate Modeling of JP-8 and of Camelina and Tallow Hydrotreated Renewable Jet Fuels at Low Temperatures. *Combust. Flame* **2013**, *160* (2), 232−239.
(17) Allen, C.; Valco, D.; Toulson, E.; Yoo, J. H.; Lee, T. JP-5 and HRJ-5 Autoignition Characteristics and Surrogate Modeling. *Energy Fuels* **2013**, *27* (12), 7790−7799.
(18) Narayanaswamy, K.; Pitsch, H.; Pepiot, P. A Component Library Framework for Deriving Kinetic Mechanisms for Multi-Component Fuel Surrogates: Application for Jet Fuel Surrogates. *Combust. Flame* **2016**, *165*, 288−309.
(19) Valco, D.; Gentz, G.; Allen, C.; Colket, M.; Edwards, T.; Gowdagiri, S.; Oehlschlaeger, M. A.; Toulson, E.; Lee, T. Autoignition Behavior of Synthetic Alternative Jet Fuels: An Examination of Chemical Composition Effects on Ignition Delays at Low to Intermediate Temperatures. *Proc. Combust. Inst.* **2015**, *35* (3), 2983−2991.

https://doi.org/10.1021/acs.energyfuels.4c01157
Energy Fuels XXXX, XXX, XXX−XXX